

# Co-channel Interference Mitigation and Cooperative Processing in Downlink Multicell Multiuser MIMO Networks

Hongyuan Zhang and Huaiyu Dai, *Member, IEEE*\*

## Abstract

Recently, the remarkable capacity potential of multiple-input multiple-output (MIMO) wireless communication systems was unveiled. The predicted enormous capacity gain of MIMO is nonetheless significantly limited by co-channel interference (CCI) in realistic cellular environments. The advanced receiver techniques proposed in [9] improve the system performance at the cost of increased receiver complexity, and the achieved system capacity is still significantly away from the interference-free capacity upper bound, especially in environments with strong CCI. In this paper, base station cooperative processing is explored to address the co-channel interference mitigation problem in downlink multicell multiuser MIMO networks, and is shown to dramatically increase the capacity with strong CCI. Both information-theoretic dirty paper coding approach and several more practical joint transmission schemes are studied, with pooled and practical per-base power constraints, respectively. Besides the CCI mitigation potential, other advantages of cooperative processing including the power gain, channel rank/conditioning advantage, and macro-diversity protection are also addressed. The potential of our proposed joint transmission schemes is verified with both heuristic and realistic cellular MIMO settings.

*Index Terms:* base station cooperation, co-channel interference, dirty paper coding, macro-diversity, rank deficiency, vector broadcast channel

---

\* The authors are with the Department of Electrical and Computer Engineering, NC State University, Raleigh, NC 27695-7511. Phone: (919) 513-0299; Fax: (919) 515-2285; Email: [hzhang@ncsu.edu](mailto:hzhang@ncsu.edu), [Huaiyu\\_Dai@ncsu.edu](mailto:Huaiyu_Dai@ncsu.edu).

## I. Introduction

In the past few years, demand for broadband wireless data access has grown exponentially. For example, existing third generation networks provide up to 2 Mb/s indoors and 144 kb/s in vehicular environments; while the minimum speed currently targeted for fourth generation systems is 10-20 Mb/s indoors and 2 Mb/s in moving vehicles. Recently, the remarkable capacity potential of multiple-input multiple-output (MIMO) systems has been unveiled [11][12]. A (flat fading) MIMO channel, typically modeled as a matrix with independent and identically distributed (i.i.d.) complex Gaussian entries, provides multiple spatial dimensions for communications and yields a spatial multiplexing gain. At high signal to noise ratio (SNR), Shannon capacity can increase linearly with the minimum number of transmit and receive antennas.

However, achieving the predicted enormous capacity gains in realistic cellular multiuser MIMO networks could be problematic. First, for realistic cellular systems, the sharing of common system resources by multiple users and the frequency reuse among adjacent cells will bring in co-channel interference (CCI), which may greatly diminish the advantages of MIMO systems [4]. Another problem in achieving these dramatic capacity gains in practice, especially for outdoor deployment, is the rank deficiency and ill-conditionness of the MIMO channel matrix. This is mainly caused by the spatial correlation due to insufficient scattering and antenna spacing [14][22], and sometimes by the “keyhole” effect even though the fading is essentially uncorrelated on each end of the channel [5]. Finally, the effect of the large-scale fading, largely neglected in current MIMO study, may also induce negative impact on the anticipated performance.

The study on the performance of interference-limited multicell multiuser MIMO attracted research attention only recently [4][2]. The study in [4] indicated the ineffectiveness of a MIMO system in an interference-limited environment, when CCI is treated as background noise. Motivated by this study, multiuser detection (MUD) and turbo decoding have been explored to significantly improve the performance of MIMO systems in a multicell structure [8][9]. Such advanced receiver techniques improve the system performance at the cost of increased receiver complexity. While they are readily applicable today at base stations (BS) or access points (AP) for uplink processing of wireless networks, they still impose challenges for the design of mobile stations (MS) in downlink communications, which is considered to be the bottleneck for next generation high-speed wireless systems. Furthermore, it is also found that there is a significant performance gap between the obtained MUD capacity and the single-cell interference-free capacity upper bound, especially in environments with strong CCI. This advocates a need to devote more system resources for performance enhancement in the downlink multicell multiuser MIMO networks.

The idea naturally arises to move the CCI mitigation to the transmitter (BS) side on the downlink, where complex structure and advanced processing can be more easily accommodated, if channel state

information (CSI) can be obtained at the transmitter side either through uplink estimation or through a feedback channel, for low user mobility scenarios such as indoor or outdoor pedestrian environments. Moreover, as multiple users in multiple cells are involved, cooperative processing at relevant base stations can be exploited. This approach is feasible, as in the current infrastructure that is common to both cellular communications and indoor wireless internet access, the base stations and access points in the system are connected by a high-speed wired backbone that allows information to be reliably exchanged among them. This approach is also reasonable, as in environments with strong interference a mobile usually experiences several *comparable* and *weak* links from surrounding radio ports, where soft handoff typically takes place in current CDMA networks. In this scenario, cooperative processing among relevant ports transforms the obstructive interference into constructive signals, which should offer large performance improvement. Joint transmitter preprocessing for single-cell multiuser MIMO communications has aroused much research interest recently (see, e.g., [1][10][26]). Base station cooperation approach is proposed in [21] to enhance the downlink sum capacity (throughput) with single-input single-output (SISO) systems employed in each cell, by implementing dirty-paper coding (DPC) proposed in [7]. In this paper, both information-theoretic DPC and some more practical joint transmission schemes will be studied with cooperative multicell base stations for downlink multiuser MIMO communications. Our analysis in general provides an upper bound for achievable performance with BS cooperation, which defines a common benchmark to gauge the efficiency of any practical scheme. The key contributions of this paper are summarized as follows.

- A common framework is proposed for the study of joint transmissions with cooperative base stations for downlink multicell multiuser MIMO networks, with both pooled and individual power constraints.
- The potential of base station cooperative processing on co-channel interference mitigation is explored from both information-theoretic and practical signal-processing standpoints, and is shown to significantly outperform the advanced receiver techniques and conventional non-cooperative signaling.
- Other advantages of base station cooperative processing are also addressed, including power gain, channel rank/conditioning advantage, and macro-diversity protection.
- Simulations results with both heuristic and realistic scenarios have been provided to demonstrate these advantages, and some practical concerns including synchronization issues are carefully addressed.

The rest of the paper is organized as follows. The system model and problem formulations are given in Section II. The concept of BS cooperation together with theoretical and practical joint transmission schemes is discussed in Section III. Other advantages of BS cooperation including power gain, rank/conditioning advantage and macro-diversity protection are further addressed in Section IV. Some

practical concerns are discussed in Section V and numerical results are provided in Section VI to verify the main points of this paper. Finally, Section VII contains some concluding remarks.

## II. System Model and Problem Formulations

Suppose in general that there are  $K$  co-channel mobile users arbitrarily distributed in the downlink multicell system, with  $N_r$  the number of receive antennas at each MS, and  $N_t$  the number of transmit antennas at each BS, respectively. Suppose that  $N_b$  is the total number of co-channel adjacent base stations in the system, so  $(N_t, N_r, N_b, K)$  can be used to represent the overall system, as in Figure 1 for a case with  $N_b = K = 3$ . With non-dispersive flat fading assumption, let  $\{\mathbf{H}_{b,j}\}_{b=1, \dots, N_b}^{j=1, \dots, K}$  be the small-scale fading channel matrix from BS  $b$  to MS  $j$ , with zero-mean unit-variance complex Gaussian entries (assuming rich scattering); and let  $\{a_{b,j}\}$  be the corresponding large-scale fading coefficients with  $a_{b,j}^2 = PL_{b,j} S_{b,j}$ , where  $PL_{b,j} = \beta_0 d_{b,j}^{-\gamma}$  represents the path loss with  $\beta_0$  a propagation constant,  $d_{b,j}$  the propagation distance,  $\gamma$  the path loss exponent, while  $S_{b,j}$  denotes the shadow fading, typically modeled as a log-normal random variable with standard deviation  $\sigma$ . Note that on the downlink, if MS  $j$  is in cell  $b$ ,  $a_{b,j} \mathbf{H}_{b,j}$  represents an in-cell channel, otherwise it is an inter-cell channel.

### A. Traditional Non-cooperative Scenario with Single-Cell Signaling

In this scenario, a mobile only communicates with its own base station, while a base station may accommodate multiple mobile users. A single-user matched filter front-end is implemented at the mobile receiver to convert the received waveform into a discrete-time signal [24]. Let  $b_j$  ( $b_j \in \{1, \dots, N_b\}$ ) represent the associated base station of user  $j$ , the equivalent discrete-time received signal of user  $j$  after matched filtering and sampling can then be expressed as:

$$\mathbf{y}_j = a_{b_j,j} \mathbf{H}_{b_j,j} \mathbf{x}_j + \sum_{k \neq j} a_{b_k,j} \mathbf{H}_{b_k,j} \mathbf{x}'_{k-j} + \mathbf{n}_j, \quad j = 1, 2, \dots, K, \quad (1)$$

where  $\mathbf{x}_j$  is the transmitted signal intended for user  $j$ , and  $\mathbf{n}_j$  is the background noise. In (1) the interference signal  $a_{b_k,j} \mathbf{H}_{b_k,j} \mathbf{x}'_{k-j}$  can come from any base station including  $b_j$  (when  $b_k = b_j$ ). We assume that the matched filter at MS  $j$  can synchronize with the signature waveform of its desired signal, but not with the waveforms of the signals intended for other users. So we use  $\mathbf{x}'_{k-j}$  to represent the equivalent discrete-time transmitted signal intended for user  $k$  and asynchronously received at MS  $j$  after matched filtering, which is a certain linear combination of two temporally consecutive symbols of  $\mathbf{x}_k$ . The background noise is assumed to be circularly symmetric complex Gaussian with covariance matrix  $\Phi_n = N_0 \mathbf{I}$ , where  $\mathbf{I}$  denotes an identity matrix. Transmit signals for all  $K$  users are assumed to be

mutually uncorrelated, and independent with the background noise. In general, a pre-processing  $N_t \times L_j$  matrix  $\mathbf{T}_j$  is applied to the transmitted data for user  $j$  as  $\mathbf{x}_j = \mathbf{T}_j \mathbf{s}_j$ , where the  $L_j \times 1$  vector  $\mathbf{s}_j$  represents the actual data intended for user  $j$ , assumed to have i.i.d. complex Gaussian entries with zero mean and unit variance ( $E(\mathbf{s}_j \mathbf{s}_j^H) = \mathbf{I}$ ). The signal intended for user  $j$  is transmitted with a power of  $E[\text{Tr}(\mathbf{x}_j \mathbf{x}_j^H)] = \text{Tr}(\mathbf{T}_j \mathbf{T}_j^H) = P_{U\_j}$ . If there is no CSI available at the transmitter, power is equally allocated among  $N_t$  transmit antennas at each BS with

$$\mathbf{T}_j = \sqrt{\frac{P_{U\_j}}{N_t}} \mathbf{I} . \quad (2)$$

Otherwise, the transmitter precoding at each BS can be designed as

$$\mathbf{T}_j = \mathbf{V}_j \mathbf{\Lambda}_j , \quad (3)$$

where  $\mathbf{V}_j$  collects the first  $L_j$  right singular vectors of the desired channel matrix  $a_{b_j,j} \mathbf{H}_{b_j,j}$ , and  $\mathbf{\Lambda}_j$  is an diagonal matrix representing the powers allocated for each eigen-mode of user  $j$  with the power constraint  $P_{U\_j}$ . To maximize the mutual information for user  $j$ , the water-filling algorithm can be used for power allocation. However, it is easy to show that equal power allocation among the  $L_j$  nonzero eigen-modes of  $a_{b_j,j} \mathbf{H}_{b_j,j}$  will result in negligible capacity loss compared to water-filling, especially at high SNR regime. Therefore the following transmit signaling is often employed for simplicity<sup>1</sup>:

$$\mathbf{T}_j = \mathbf{V}_j \sqrt{\frac{P_{U\_j}}{L_j}} \mathbf{I} . \quad (4)$$

A lower bound for single-cell signaling schemes can be derived with the conventional single user detector, which simply treats CCI as additive white Gaussian noise. The spectral efficiency for user  $j$  with this conventional single user detector is then given by [8]

$$R_{j\_conv} = \log \left| \mathbf{I} + \frac{a_{b_j,j}^2}{(N_0 + \sum_{k \neq j} P_{U\_k} a_{b_k,j}^2)} \mathbf{H}_{b_j,j} \mathbf{T}_j \mathbf{T}_j^H \mathbf{H}_{b_j,j}^H \right| , \quad (5)$$

in which  $\mathbf{T}_j$  can be designed using (2)~(4) based on the availability of CSI at the transmitter. On the other hand, the single-cell signaling interference-free upper bound unrealistically assumes no interference at the receiver of MS  $j$ :

---

<sup>1</sup> Note that signaling (4) is equivalent to (2) for full rank channels, but significantly different otherwise.

$$R_{j\_single\ cell} = \log \left| \mathbf{I} + \frac{a_{b_j,j}^2}{N_0} \mathbf{H}_{b_j,j} \mathbf{T}_j \mathbf{T}_j^H \mathbf{H}_{b_j,j}^H \right| = \sum_{l=1}^{L_j} \log \left( 1 + \frac{P_l}{N_0} \lambda_l^2 \right), \quad (6)$$

where the second equality follows from the singular value decomposition (SVD) of  $a_{b_j,j} \mathbf{H}_{b_j,j}$ .

The receiver MUD schemes proposed in [8] and [9], including the group linear minimum-mean-square-error (MMSE) detector, the group MMSE successive interference cancellation (SIC) detector and the adaptive multiuser detector, can improve the performance of MIMO systems in a multicell structure. However, they require MS  $j$  to know not only its desired channel, but also the interfering channels, and some receivers may need to detect both the desired and interfering signals. They can be readily implemented at BS for CCI mitigation on the uplink, but may still be impractical for current MS on the downlink because of their complexity. Furthermore, it is found in [8] and [9] that the performances of the multiuser receivers are still far from the interference-free upper bound (6), especially in environments with strong interference, which indicates a need to exploit more system resources for throughput enhancement.

## B. BS Cooperation Scenario

For BS cooperation schemes, the transmit signal for each user is spread over all  $N_b$  base stations. Then  $\mathbf{x}_j = [\mathbf{x}_j^{[1]T}, \mathbf{x}_j^{[2]T}, \dots, \mathbf{x}_j^{[N_b]T}]^T$ , where  $\mathbf{x}_j^{[b]}$  is the transmitted signal intended for user  $j$  from BS  $b$ . With the assumption that the transmitter knows the propagation delay for each BS-MS pair,  $\mathbf{x}_j$  can be pre-compensated for the different delays from different base stations to MS  $j$ . So MS  $j$  can still receive a synchronized  $\mathbf{x}_j$ :

$$\mathbf{y}_j = \mathbf{H}_{Ej} \mathbf{x}_j + \sum_{k \neq j} \mathbf{H}_{Ej} \mathbf{x}'_{k-j} + \mathbf{n}_j, \quad (7)$$

where  $\mathbf{H}_{Ej} = [a_{1,j} \mathbf{H}_{1,j}, a_{2,j} \mathbf{H}_{2,j}, \dots, a_{N_b,j} \mathbf{H}_{N_b,j}]_{N_r \times N_t N_b}$ , (8)

and in  $\mathbf{x}'_{k-j} = [\mathbf{x}_{k-j}^{[1]T}, \mathbf{x}_{k-j}^{[2]T}, \dots, \mathbf{x}_{k-j}^{[N_b]T}]^T$ ,  $\mathbf{x}'_{k-j}$  represents asynchronous reception of  $\mathbf{x}_k^{[b]}$  at MS  $j$ , given that  $\mathbf{x}_k$  cannot be pre-compensated for MS  $j$  during joint transmission. In this scenario, the transmit matrix  $\{\mathbf{T}_j\}$  are of the dimension  $N_t N_b \times L_j$ , and  $\{\mathbf{T}_j\}_{j=1}^K$  are designed only based on the characteristics of  $\{\mathbf{H}_{Ej}\}_{j=1}^K$ , which are assumed to be constant over a much longer period than the largest delay among all BS-MS pairs in the system, with the quasi-static fading channel assumption. So  $\{\mathbf{T}_j\}$  are constant during this time period and we have  $\mathbf{x}'_{k-j} = \mathbf{T}_k \mathbf{s}'_{k-j}$ , where  $\mathbf{s}'_{k-j} = [\mathbf{s}_{k-j}^{[1]T}, \mathbf{s}_{k-j}^{[2]T}, \dots, \mathbf{s}_{k-j}^{[N_b]T}]^T$ , and  $\mathbf{s}_{k-j}^{[b]}$  is the corresponding asynchronous reception of the sub-streams in  $\mathbf{s}_k$  transmitted from BS  $b$ , as discussed above. Therefore, (7) can be re-written as

$$\mathbf{y}_j = \mathbf{H}_{Ej} \mathbf{T} \mathbf{s}_{[j]} + \mathbf{n}_j, \quad (9)$$

where  $\mathbf{T} = [\mathbf{T}_1, \mathbf{T}_2, \dots, \mathbf{T}_K]_{N_t N_b \times \sum_k L_k}$ , and  $\mathbf{s}_{[j]}^T = [\mathbf{s}'_{1-j}{}^T, \dots, \mathbf{s}'_{j-1-j}{}^T, \mathbf{s}'_j{}^T, \mathbf{s}'_{j+1-j}{}^T, \dots, \mathbf{s}'_{K-j}{}^T]_{\sum_k L_k \times 1}$ . For

simplicity, we still assume that  $\{\mathbf{s}'_{k-j}\}$  have i.i.d. complex Gaussian entries with zero mean and unit variance.

The key problem of joint transmit processing among cooperative base stations is to jointly design a transmit matrix  $\mathbf{T}$  to mitigate co-channel interference and enhance the system spectral efficiency with either a pooled power constraint:

$$\mathbb{E}[\sum_{k=1}^K \text{Tr}(\mathbf{x}_k \mathbf{x}_k^H)] = \text{Tr}(\sum_{k=1}^K \mathbf{T}_k \mathbf{T}_k^H) \leq P_t, \quad (10)$$

or more practical per-base power constraints:

$$\mathbb{E}[\sum_{k=1}^K \text{Tr}(\mathbf{x}_k^{[b]} \mathbf{x}_k^{[b]H})] = \text{Tr}(\mathbf{T}^{[b]} \mathbf{T}^{[b]H}) = \text{Tr}(\sum_{k=1}^K \mathbf{T}_k^{[b]} \mathbf{T}_k^{[b]H}) \leq P_{B\_b}, \quad b = 1, 2, \dots, N_b, \quad (11)$$

where  $\mathbf{T}^{[b]}$  and  $\mathbf{T}_k^{[b]}$  are the rows in  $\mathbf{T}$  and  $\mathbf{T}_k$  corresponding to the transmit antennas at BS  $b$ , respectively. In our study, since MS  $j$  is not interested in correctly detecting  $\mathbf{s}_k$ , for  $k \neq j$ , the design of the joint transmit matrix  $\mathbf{T}$  is actually not affected by the asynchronous receptions of interfering signals and  $\{\mathbf{s}'_{k-j}\}$  can be simply viewed as the data of some virtual synchronous interfering users.

### III. Joint Transmission Techniques with Base Station Cooperation

As seen in Figure 1, by cooperating the  $N_b$  adjacent base stations, the downlink of a  $(N_t, N_r, N_b, K)$  multicell multiuser MIMO system forms a vector broadcast channel (BC), in which the  $NT = N_t \times N_b$  transmit antennas are distributed among the  $N_b$  radio ports (or base stations). Unlike traditional BC with co-located MIMO channels, the channel gains from any two antenna elements at different BS are independent. With base station cooperation, the system resources can be pooled together for more efficient use. In particular, the severe CCI problem can be effectively controlled and significant performance improvement can be achieved. Meanwhile, the complexity at MS can be significantly reduced.

In the following, the potential of cooperative processing for system capacity enhancement is first studied from a theoretical standpoint, by extending the dirty paper coding approach with a pooled power constraint (10) to the downlink multicell multiuser scenario. Then some more practical suboptimal transmission schemes, with more practical per-base power constraints (11), will also be investigated.

#### A. Performance Upper Bound: Dirty Paper Coding with Pooled Power Constraint

For a system with perfect data and power cooperation among  $N_b$  base stations, we can implement the throughput-achieving dirty paper coding [7][12], at the vector broadcast channel formed by cooperative BSs, to obtain a system performance upper bound. Note that with the asynchronous vector BC model (7), we apply DPC in a slightly different way, where the encoder for the “current” user needs to non-causally know not only the encoding of “previous” users and associated CSI, but also the corresponding propagation delays, to pre-cancel the interference from “previous” users. The rate of each user and the (optimal) sum rate can then be expressed as:

$$R_{\pi(j)\text{-DPC}}(\mathbf{T}) = \log \frac{\left| N_0 \mathbf{I} + \mathbf{H}_{E\pi(j)} \left( \sum_{k \geq j} \mathbf{T}_{\pi(k)} \mathbf{T}_{\pi(k)}^H \right) \mathbf{H}_{E\pi(j)}^H \right|}{\left| N_0 \mathbf{I} + \mathbf{H}_{E\pi(j)} \left( \sum_{k > j} \mathbf{T}_{\pi(k)} \mathbf{T}_{\pi(k)}^H \right) \mathbf{H}_{E\pi(j)}^H \right|}, \quad (12)$$

$$SR_{DPC} = \max_{\text{Tr}(\mathbf{T}\mathbf{T}^H) = P_t, \pi} \left( \sum_{\pi(j)} R_{\pi(j)\text{-DPC}}(\mathbf{T}) \right), \quad (13)$$

where  $\mathbf{T}$  is given in (9), and  $\pi(1), \pi(2), \dots, \pi(K)$  represents a certain user ordering. By applying the duality of the broadcast and multiple-access channels (MAC) [18], (13) can be obtained by calculating the sum rate of a dual MAC with the same total power constraint  $P_t$ . Iterative numerical methods that jointly optimize (13) on the dual uplink were proposed (see e.g. [17] and [29]) based on the iterative water-filling algorithm proposed in [28]. Furthermore, it is shown that (13) is actually the saddle point (with worst-case colored noise) of the Sato’s bound, which is the sum rate of a heuristic cooperative system where both transmitters and receivers can cooperate with each other, given by [20]:

$$SR_{Sato} = \max_{\text{Tr}(\mathbf{T}\mathbf{T}^H) \leq P_t} \log \frac{\left| \Phi_n + \mathbf{H}_T \mathbf{T} \mathbf{T}^H \mathbf{H}_T^H \right|}{\left| \Phi_n \right|}, \quad (14)$$

where  $\mathbf{H}_T = [\mathbf{H}_{E1}^T, \mathbf{H}_{E2}^T, \dots, \mathbf{H}_{EK}^T]^T$  and  $\Phi_n$  is the noise covariance matrix.

In [21], the concept of DPC on cooperative BS is proposed with a simple scalar channel for each cell. A suboptimal algorithm, dirty paper coding with linear pre-processing (LP-DP), is exploited to simplify the optimization procedure involved in (13), with a negligible performance penalty. It is also proved that LP-DP is asymptotically optimal at high SNR [3]. For the special case of  $K = N_b$ , we can extend LP-DP to our multicell MIMO vector BC scenario as in Appendix A. In short, by applying LQ decompositions and DPC, we can get  $K$  parallel interference-free channels for the  $K$  users, with the sum rate:

$$SR_{LPDP} = \sum_{j=1}^K \sum_{l=1}^{L_j} \log \left| 1 + \frac{P_{j,l} \lambda_{j,l}^2}{N_0} \right|, \quad (15)$$

where  $P_{j,l}$  and  $\lambda_{j,l}$  are the allocated power and singular value for the  $l$ th non-zero eigen-mode of user  $k$ ’s virtual interference-free channel, respectively.

DPC with per-base constraints is much more involved, as the MAC/BC duality does not hold any more. DPC has not been shown to achieve the capacity region or even the sum capacity with constraints (11). Complex iterative multistage numerical methods for cooperative DPC with constraints (11) are proposed in [12][15][16], in which a small piece of power is invested to a certain selected user until one of the BS reaches its power constraint. The path gains corresponding to this BS are then set to zero in subsequent stages so that no further power is allocated to these antennas. In general, (11) is more strict than (10), so a performance degradation is expected.

Although the DPC scheme with a pooled power constraint gives us a simple performance upper bound for BS cooperation, some unrealistic assumptions are made, such as the non-causal knowledge of interference sequence at the transmitter, which motivates the exploration of more practical joint transmission schemes, as will be discussed in the following.

### B. Suboptimal Joint Transmission Schemes for BS Cooperation with Per-Base Power Constraints

DPC is an information theoretical approach that can demonstrate the potential of joint transmission with cooperative processing. In this part, several suboptimal but more practical joint transmission schemes with the more practical per-base power constraints are exploited for better understanding of the achievable performance gains of BS cooperative processing in practice. Essentially these techniques are counterparts of corresponding multiuser detectors, some of which have been revisited in the co-located MIMO context recently [1][6][23]. These suboptimal joint transmission schemes will be compared with both the receiver MUD approaches [8][9] and DPC approaches in Section VI. A. In general, the following expression holds true for the spectral efficiencies of user  $j$  with these joint linear transmission schemes (except TDMA):

$$R_{j\_subopt}(\mathbf{T}) = \log \left| \mathbf{I} + [N_0 \mathbf{I} + \mathbf{H}_{Ej} (\sum_{i \neq j} \mathbf{T}_i \mathbf{T}_i^H) \mathbf{H}_{Ej}^H]^{-1} \mathbf{H}_{Ej} \mathbf{T}_j \mathbf{T}_j^H \mathbf{H}_{Ej}^H \right|, \quad (16)$$

where different schemes correspond to different choices of transmission matrices  $\{\mathbf{T}_j\}$  or  $\mathbf{T}$  with the constraints (11). As discussed in Section II, the design of  $\{\mathbf{T}_j\}$  only depends on  $\{\mathbf{H}_{Ej}\}$ , but not on the transmitted signals, so the asynchronous receptions in (7) assume no influence on such designs, if pre-compensation for each user's data is implemented at the joint transmitter. Intuitively, compared with DPC, (16) may induce more transmit power inefficiency, as  $\mathbf{T}$  is responsible for the mitigation of interference from both "previous" and "subsequent" users, and per-base power constraints are implemented instead of a pooled power constraint.

Before discussing these suboptimal joint transmission schemes in detail, we first propose a simple algorithm for designing  $\mathbf{T}$  with per-base power constraints. Let  $L_T = \sum_{k=1}^K L_k$  be the overall number of data streams of  $K$  users. Suppose that a preliminary joint linear transmit matrix  $\mathbf{G}_{N_b N_s \times L_T}$  is given, whose designs will be introduced in the sequel. Our design of  $\mathbf{T}$  with per-base power constraints (11) is given by

$$\mathbf{T} = \mathbf{G}\mathbf{\Omega}, \quad (17)$$

where  $\mathbf{\Omega}$  is a  $L_T \times L_T$  diagonal matrix with diagonals  $\{\mu_l\}_{l=1}^{L_T}$  each representing the allocated power for the corresponding original data stream. Since typically  $L_T \gg N_b$  and there are only  $N_b$  per-base power constraints in (11), we can further divide  $\{\mu_l\}_{l=1}^{L_T}$  into  $N_b$  groups each with  $L_T / N_b$  elements having the same value:

$$\mathbf{\Omega} = \text{blockdiag}(\mu_1 \mathbf{I}, \mu_2 \mathbf{I}, \dots, \mu_{N_b} \mathbf{I}). \quad (18)$$

Further define

$$\mathbf{Q}_{N_b \times N_b} = \begin{bmatrix} \|\mathbf{G}_1^{[1]}\|_F^2 & \|\mathbf{G}_2^{[1]}\|_F^2 & \dots & \|\mathbf{G}_{N_b}^{[1]}\|_F^2 \\ \|\mathbf{G}_1^{[2]}\|_F^2 & \|\mathbf{G}_2^{[2]}\|_F^2 & \dots & \|\mathbf{G}_{N_b}^{[2]}\|_F^2 \\ \vdots & \vdots & \vdots & \vdots \\ \|\mathbf{G}_1^{[N_b]}\|_F^2 & \|\mathbf{G}_2^{[N_b]}\|_F^2 & \dots & \|\mathbf{G}_{N_b}^{[N_b]}\|_F^2 \end{bmatrix}, \quad (19)$$

where  $\mathbf{G}_j^{[b]}$  is an  $N_t \times L_T / N_b$  submatrix in  $\mathbf{G}$ , corresponding to the transmit weights at BS  $b$  for the  $j$ th group of data streams as defined above. Let  $\mathbf{P} = [P_{B-1}, P_{B-2}, \dots, P_{B-N_b}]^T$  be the per-base power constraint vector, then we can calculate  $\mathbf{\Omega}$  by solving the linear system equation:

$$\boldsymbol{\mu} = [\mu_1^2, \mu_2^2, \dots, \mu_{N_b}^2]^T = \mathbf{Q}^{-1} \mathbf{P}. \quad (20)$$

When an infeasible solution ( $\boldsymbol{\mu}$  does not have all positive entries) is obtained, we can refine it as:

$$\mathbf{\Omega} = \mu \mathbf{I}, \quad \mu = \min_{b=1,2,\dots,N_b} \left( \frac{P_{B-b}}{\|\mathbf{G}^{[b]}\|_F^2} \right), \quad (21)$$

where  $\mathbf{G}^{[b]}$  is the rows of  $\mathbf{G}$  corresponding to transmit antennas at BS  $b$ . Note that (20) can utilize the full power at each BS, while in (21) only the BS satisfying the minimum value can transmit with full power and any other BS transmits with a power less than its power constraint. Nonetheless, it has been shown that designs with per-base power constraints incur insignificant performance loss for linear joint transmission schemes compared to the corresponding designs with pooled power constraint, thus demonstrating the applicability of these joint transmission schemes in realistic cellular communications. These suboptimal schemes are illustrated as follows.

**TDMA:** The simplest way of totally eliminating CCI is to implement time-division multiple-access (TDMA) in the multicell downlink. At each time slot, the network services one single user, and all the antenna elements and transmit power are employed for such transmission, with the pre-compensation of different delays. The spectral efficiency of user  $j$  with joint TDMA signaling is then given by:

$$R_{j\_TDMA} = \frac{1}{K} \log \left| \mathbf{I} + \mathbf{H}_{Ej} \mathbf{T} \mathbf{T}^H \mathbf{H}_{Ej}^H \right|, \quad (22)$$

with the joint transmission matrix  $\mathbf{T} = \mathbf{G} \cdot \boldsymbol{\Omega}$  exclusively designed for user  $j$ . During the time slot for user  $j$ , the preliminary transmission matrix can be expressed by  $\mathbf{G} = [\mathbf{0}, \mathbf{0}, \dots, \mathbf{V}_j, \dots, \mathbf{0}]$ , in which  $\mathbf{V}_j$  collects the first  $L_j$  right singular vectors of  $\mathbf{H}_{Ej}$ . Since (19) is singular, the diagonal matrix  $\boldsymbol{\Omega}$  is calculated by (21) to satisfy the per-base power constraint as discussed above. As is already known, from the system capacity viewpoint, it is beneficial to serve multiple users simultaneously and actively control the CCI rather than to allow one single user occupy the whole system resource exclusively. This is also verified from our numerical results in Section VI. A.

**Single User Eigen-Beamforming:** This approach can be viewed as the counterpart of the conventional single user detector (see (5)), which implements eigen-beamforming for each user with respect to the corresponding channel matrix without considering the CCI. Thus we have  $\mathbf{G}_j = \mathbf{V}_j$ , where  $\mathbf{V}_j$  is defined as in the TDMA scheme, and  $\mathbf{G} = [\mathbf{G}_1, \mathbf{G}_2, \dots, \mathbf{G}_K]$ . Compared with single-cell signaling systems, this scheme only achieves a power gain, which will be introduced in Section IV. A.

**Joint Transmitter Zero Forcing (JT-ZF):** This approach can be viewed as the counterpart of the multiuser decorrelator, which employs a pseudo-inverse of  $\mathbf{H}_T = [\mathbf{H}_{E1}^T, \mathbf{H}_{E2}^T, \dots, \mathbf{H}_{EK}^T]^T$  with

$$\mathbf{G} = \mathbf{H}_T^H (\mathbf{H}_T \mathbf{H}_T^H)^{-1}, \quad \mathbf{T}_j = \mathbf{G}_j \cdot \boldsymbol{\Omega}_j, \quad (23)$$

where  $\boldsymbol{\Omega}_j$  is the corresponding  $j$ th  $L_j \times L_j$  diagonal block of  $\boldsymbol{\Omega}$ . With this approach, we can easily get

$\mathbf{H}_{Ej} \cdot \mathbf{T}_i = \begin{cases} \boldsymbol{\Omega}_i \mathbf{I}, & i = j \\ \mathbf{0}, & i \neq j \end{cases}$ . Then (7) can be re-written as  $\mathbf{y}_j = \boldsymbol{\Omega}_j \mathbf{s}_j + \mathbf{n}_j$ , and interference from both other

users and other sub-streams of the same user are eliminated simultaneously. Just as ZF receivers eliminate the interference at the expense of noise enhancement, ZF transmitters generally increase the average transmit power by the same factor. Furthermore, in the rank deficient scenario where  $\mathbf{H}_T \mathbf{H}_T^H$  is singular, this approach cannot even be applied. These observations naturally motivate the joint transmission design based on MMSE criterion.

**Joint Transmitter MMSE (JT-MMSE):** Recalling the trade-off between interference cancellation and noise enhancement for its receiver counterpart, JT-MMSE makes a good trade-off between interference cancellation and transmitter power efficiency, whose preliminary joint transmission matrix is given as

$$\mathbf{G} = \mathbf{H}_T^H \left( \mathbf{H}_T \mathbf{H}_T^H + \frac{N_0}{P_t} \mathbf{I} \right)^{-1}. \quad (24)$$

**Joint Transmitter Null-space Decomposition (JT-Decomp):** For this approach, the preliminary transmission matrix for user  $j$  can be described as:

$$\mathbf{G}_j = \bar{\mathbf{V}}_j \mathbf{V}_j', \quad (25)$$

where  $\bar{\mathbf{V}}_j$  includes the right singular vectors corresponding to the null space (zero singular values) of  $\bar{\mathbf{H}}_{T\_j} = [\mathbf{H}_{E1}^T, \dots, \mathbf{H}_{Ej-1}^T, \mathbf{H}_{Ej+1}^T, \dots, \mathbf{H}_{EK}^T]^T$ , and  $\mathbf{V}_j'$  includes the first  $L_j$  right singular vectors of the virtual channel  $\mathbf{H}_{Ej}' = \mathbf{H}_{Ej} \bar{\mathbf{V}}_j$ .  $\bar{\mathbf{H}}_{T\_j}$  usually has a non-zero null space, so  $\mathbf{H}_{Ei} \bar{\mathbf{V}}_j = \mathbf{0}$ ,  $i \neq j$  can be guaranteed. Interference from all other users is cancelled, and we obtain a set of equivalent parallel interference-free subchannels  $\{\mathbf{H}_{Ej}'\}$ .

JT-Decomp approach generally outperforms JT-MMSE and JT-ZF at the cost of extra complexity, as will be seen in our numerical results. There is again a potential problem with this approach in the rank deficient scenario. If  $\mathbf{H}_{Ej}$  is rank deficient, there will be a higher chance that  $\text{null}(\bar{\mathbf{H}}_{T\_j})$  overlaps with  $\text{null}(\mathbf{H}_{Ej})$ , which means that the equivalent channel  $\mathbf{H}_{Ej}'$  may have reduced channel rank or even null rank (when  $\text{null}(\bar{\mathbf{H}}_{T\_j}) = \text{null}(\mathbf{H}_{Ej})$ ). Fortunately, as we will illustrate in the next section, this will rarely happen in our distributed multicell MIMO setting, as compared to the traditional co-located MIMO.

## IV. Other Advantages of Base Station Cooperation

With base station cooperation, all antennas of the relevant multicell base stations can be jointly employed for data processing and transmission. In some sense, it is equivalent to a single giant base station or processing center. The key differences from the single-cell scenario with co-located antennas at one BS, are the widely distributed antennas and independent large-scale fading experienced for each link between a mobile-port pair. Besides its potential in CCI cancellation, base station cooperative processing assumes other advantages in multicell MIMO communications, as indicated below.

### A. Power Gain

Considering a single user interference-free channel with a transmit power constraint  $P_{U\_j}$ , with BS cooperation, the channel changes from a  $N_r \times N_t$  matrix  $a_{b_j,j} \mathbf{H}_{b_j,j}$  to a  $N_r \times N_t N_b$  matrix  $\mathbf{H}_{Ej}$ , so we get a channel power gain. Typically  $N_t$  is larger than  $N_r$  on the downlink, so both matrices have a rank of  $N_r$  in rich scattering environment. From the single user spectral efficiency expression (6), based on the fact that  $\sum_i \lambda_i^2 = \|\mathbf{H}\|_F^2$ , it is easily seen that with the same channel rank, power constraint, and power allocation algorithm, the higher the channel power, the larger the spectral efficiency. Specifically, the equivalent single user channel power for single-cell interference-free channel  $a_{b_j,j} \mathbf{H}_{b_j,j}$  is given

by  $a_{b_j,j}^2 E[\|\mathbf{H}_{b_j,j}\|_F^2] = a_{b_j,j}^2 N_t N_r$ , while the single user channel power with BS cooperation is given by

$$E[\|\mathbf{H}_{Ej}\|_F^2] = (a_{b_j,j}^2 + \sum_{b \neq b_j} a_{b,j}^2) N_t N_r. \text{ Note that by comparing the above two equations, the relative}$$

power gain is significant if MS  $j$  has comparable links to adjacent base stations, which represents a strong CCI case. It will typically result in a parallel shift of the spectral efficiency versus SNR curve at high SNR.

In general, for joint transmission schemes, transmit matrix  $\mathbf{T}$  uses a portion of the total power for interference mitigation, and the per-base power constraint (11) may also reduce the available power. Such transmit power inefficiency may compromise the power gain achieved by BS cooperation. This effect is sometimes eminent for suboptimal linear joint transmission schemes in Section III. B, as will be shown in the numerical results of Section VI. A.

## B. Channel Rank and Conditioning Advantages

The capacity of a MIMO system is determined by the characteristics of the channel matrix  $\mathbf{H}$ . Clearly  $r = \text{rank}(\mathbf{H})$  is one such important factor, which determines the number of parallel sub-channels that can be opened up for independent communications. In rich-scattering environments, full rank can be assumed and essentially  $r = \min(N_t, N_r)$  more bits/s/Hz are obtained for every 3 dB increase in power. However, in some extreme environments (e.g., the keyhole problem [5]), a MIMO system will lose its capacity advantage (spatial multiplexing gain) over a SISO system, even though other advantages like diversity and array gains may still preserve. Another important factor influencing the MIMO capacity is the channel condition number  $\kappa = \frac{\max_i \lambda_i}{\min_i \lambda_i}$ , or more generally the singular value distribution of the channel

matrix. Noting that equal power allocation achieves optimal performance at high SNR in the full channel rank case, we conclude from (6) by Jensen's inequality that a channel with  $\kappa = 1$  has the largest capacity, with the same power constraint. In rich scattering environment, channel matrix  $\mathbf{H}$  is assumed to have normalized i.i.d. complex Gaussian entries and thus is well-conditioned. In realistic environments,  $\mathbf{H}$  may get ill-conditioned due to fading correlation, resulting from the existence of few dominant scatterers, small angle spread, and insufficient antenna spacing [22]. From (6) we see that those sub-channels with  $\lambda_i^2 \ll 1$  are essentially of no use, even though the channel still has a full rank.

In a typical outdoor urban scenario, antenna arrays at the base stations are elevated above urban clusters and far away from local scattering, while mobile terminals are surrounded by rich scatterers, and the number of independent paths is limited by few far-field reflectors [14]. Therefore, the downlink channel matrix with co-located transmit array can be modeled as

$$\mathbf{H} = c \mathbf{H}_w \mathbf{A}_t^H, \quad (26)$$

where  $\mathbf{A}_t$  collects the dominant transmit array response vectors,  $\mathbf{H}_w$  is a normalized white Gaussian matrix, and  $c$  is the normalization factor. In this case, the channel matrix may be both rank-deficient and ill-conditioned, determined by the propagation and system parameters.

For BS cooperation in multicell MIMO, the overall transmit array is distributed among cooperative base stations, so in the equivalent channel for user  $j$   $\mathbf{H}_{Ej} = [a_{1,j}\mathbf{H}_{1,j}, a_{2,j}\mathbf{H}_{2,j}, \dots, a_{N_b,j}\mathbf{H}_{N_b,j}]$ ,  $\{\mathbf{H}_{b,j}\}_{b=1}^{N_b}$  (all modeled as (26) for outdoor deployment) are independent with each other. The overall number of independent links is then given by  $\sum_{b=1}^{N_b} \text{rank}(\mathbf{H}_{b,j})$ , which is guaranteed to be at least equal to  $N_b$ . If  $N_b \geq N_r$ ,  $\mathbf{H}_{Ej}$  will always have a full rank. Furthermore, the channel conditioning will not be greatly degraded even if transmit fading correlation happens at each base station, as the fading between different transmit antennas at different base stations are still uncorrelated.

Because of the channel rank and conditioning advantages with BS cooperation, joint transmission schemes in Section III will not significantly degrade, compared to single-cell signaling with co-located antennas. In particular, the chance that JT-ZF cannot be implemented, or the chance that  $\text{null}(\overline{\mathbf{H}}_{T_i})$  overlaps with  $\text{null}(\mathbf{H}_{Ei})$  for JT-Decomp (refer to Section III.B), will be greatly reduced. These suboptimal joint transmission schemes will be shown to even outperform the single-cell upper bound at high SNR for rank deficient channels.

### C. Macro-diversity Protection for Shadowing Channels

Shadowing in wireless channels is a position sensitive factor, which means that signals from transmit antennas co-located at the same base station are generally subject to the same shadowing, while those from different base stations subject to independent shadowing. Under severe shadowing, the capacity of a single cell MIMO with co-located antennas will degrade significantly. On the other hand, cooperative BSs can provide the macro-diversity protection for shadowing impairment, because of their independency. Intuitively, the probability that all sub-channels of  $\mathbf{H}_{Ej}$  are under deep shadow fading is much lower than a co-located MIMO channel. Macro-diversity cannot increase the mean of the received SNR, but will greatly reduce its variance. This resulting gain with respect to the outage capacity will be demonstrated in Section VI C.

## V. Some Practical Concerns

Previous studies, such as those in [12][15][16][21], ignored the issues of asynchronous receptions for tractable analysis. In our study, we assume that the cooperative base stations can pre-compensate different delays in  $\mathbf{x}_j$ , which results in its synchronous reception at MS  $j$ ; while interfering signals are still received asynchronously. However, for some scenarios involving fast fading and/or high mobility, the

pre-compensation may require too much system resource. When such joint synchronization among different base stations is not available, we can then either implement more complex signal processing based on asynchronous system models, which directs our future research; or simply restrict our attention to the scenario where co-channel users are all around the cell borders (e.g. around point **A** in Figure 1) where soft-handoff takes place, so that the synchronous receptions of both desired and interfering signals can be assumed. To summarize, our analysis in general provides an upper bound for achievable performance with BS cooperation, which defines a common benchmark to gauge the efficiency of any practical schemes. This upper bound becomes rather tight when joint synchronization among different base stations is available through, e.g., GPS devices. Clearly the system performance is improved at the cost of significant system overhead related to CSI feedback and information exchange, which should be carefully justified in specific scenarios.

## VI. Numerical Results

In this section, simulation results are presented for both heuristic and practical cellular scenarios, to fully demonstrate the potential of BS cooperation processing in downlink multicell multiuser MIMO networks. VI.A~VI.C simulate an ideal symmetric strong CCI scenario, which is similar to the Wyner's model [27][21], and reveals the achievable performance bounds for BS cooperative processing schemes; while VI.D investigates the performance advantage of BS cooperation over traditional single-cell signaling schemes in a realistic cellular scenario.

### A. Performance under Rayleigh Fading

A simple *symmetric* three-cell scenario, (2,2,3,3) multicell MIMO network with three co-channel users located in three different cells (Figure 1) is considered, which may represent TDMA, FDMA, or orthogonal CDMA. We also assume that  $a_{b,j}^2 = 0.5$  (no shadowing),  $\forall b \neq j$ , normalized with respect to the in-cell large-scale fading  $\{a_{b,j}^2\}_{j=1}^3 = 1$  without loss of generality, which represents a strong CCI scenario. For single-cell signaling schemes, data for each user is transmitted with an identical power  $\{P_{U_j}\}_{j=1}^K = P$ . Rayleigh fading is assumed. Optimal DPC (13) is obtained through the numerical algorithm in [17], and LP-DP is implemented according to Appendix A. Pooled power constraint is imposed for DPC schemes with  $P_t = 3P$ , while per-base constraints (11) are enforced for all the other suboptimal BS cooperation schemes. The sum rates of BS cooperation schemes and Sato's bound are divided by three to represent the average rate per user, for a fair comparison with the single-cell signaling schemes. Also, the lower and upper bounds in single-cell approaches, (5) and (6), and the spectral efficiency of the optimal multiuser receiver from [8] are given for reference. The rate curves averaged

over all fading states (ergodic rates) are plotted in Figure 2 with respect to average transmit SNR per user, given as  $\rho = P/N_0$ .

From Figure 2, we see that the performance of the optimal multiuser receiver is still significantly away from the single-cell upper bound. On the other hand, the DPC schemes for BS cooperation result in a significant performance gain over the multiuser receivers, and they even outperform the single-cell upper bound and approach the Sato's upper bound at high SNR. Particularly, the approximate 2 bits/s/Hz gap between the Sato's Bound (as well as DPC schemes) and single-cell upper bound at high SNR, which is resulted from the power gain, can be verified through their equivalent channel power evaluation (see Appendix B).

As discussed in Section IV. A, suboptimal joint transmission schemes reduce interference at the expense of transmitter power inefficiency, which may compromise the power gain and may result in a performance worse than the single-cell interference-free upper bound. This can be observed in Figure 2. Nonetheless, all these suboptimal joint transmission schemes except the single user eigen-beamforming significantly outperform the multiuser receivers, thus verifying the capability of BS cooperation in practical deployment. Furthermore, from Figure 2 we can see that the JT-Decomp approach outperforms JT-MMSE at the cost of extra complexity, and that JT-ZF converges to JT-MMSE at high SNR, which is a well-known result. TDMA performs worse than JT-ZF at high SNR, where JT-ZF's interference cancellation advantage becomes more eminent, which confirms our previous prediction.

It is not difficult to prove that power gain is the major factor influencing the spectral efficiency at low SNR. Therefore, the single user eigen-beamforming with BS cooperation is better than the receiver MUD at low SNR, because of its power gain; but gets worse at high SNR, because it does not actively mitigate the interference. The gap between the single user eigen-beamforming with BS cooperation and the conventional single user detector is the same as the gap between Sato's bound and single-cell upper bound due to the power gain.

## B. Rank Deficient Case

Now we use the same parameter setting as in part VI.A, except that the channel model of (26) is used for  $\{\mathbf{H}_{b,j}\}$  with one dominant path, so the ranks of  $\{\mathbf{H}_{b,j}\}$  are one. From Figure 3, we can see that the spectral efficiencies of single-cell signaling schemes and the single-cell upper bound degrade (cf. Figure 2) because of the reduced channel rank. Notice that different rank results in different slopes of the rate curves. From Figure 3, we can see that there is a 2 more bits/s/Hz spectral efficiency gain for every 3dB transmit SNR increase for BS cooperation schemes, while there is only a 1 bits/s/Hz gain with the same transmit SNR increase for the single-cell upper bound. That is why JT-ZF and JT-Decomp can even outperform the single-cell upper bound at high SNR, as the spatial multiplexing gain compensates the power inefficiency. Thanks to channel rank and conditioning advantages with BS cooperation,

performances of all joint transmission schemes don't deteriorate significantly in this deficient channel (cf. Figure 2), including the otherwise problematic JT-ZF and JT-Decomp schemes.

### C. Macro-diversity

In this simulation, besides the path loss as defined in VI.A, shadowing effect is considered for  $\{a_{b,j}\}$ , which are independent for different base stations.  $p = 10\%$  outage capacity is evaluated, for the same symmetric (2,2,3,3) symmetric scenario as above. In Figure 4, we compare the outage spectral efficiency of the single-cell interference-free upper bound, with that of the BS cooperation scheme JT-Decomp (25), with the shadowing standard deviation  $\sigma$  ranging from 6dB to 15dB. Rayleigh fading is again assumed for  $\{\mathbf{H}_{b,j}\}$ . Because of the macro-diversity protection, we can see that the outage spectral efficiency of JT-Decomp is much more robust than that of the single-cell upper bound when subject to shadow fading, outperforming it at severe shadowing scenarios.

### D. Simulation of a Realistic Cellular Scenario

We now further consider a more realistic (2,2,3,3) system, in which users with low mobility can be arbitrarily located, so that average CCI for each user will be reduced compared with the scenario assumed in VI.A~VI.C. Suppose that in a realistic downlink scenario as in Figure 5, three base stations use the same frequency band. By using 120-degree sectoring in each cell, we are interested only in the shadowed area, in which three users are uniformly distributed. The radius of each cell is 1000m, which represents an urban scenario. We only consider the interference from three base stations. Signals from other far-away base stations can be approximately treated as additive white Gaussian noise. Rayleigh fading is assumed for small-scale fading. For the large-scale fading  $a_{b,j}^2 = PL_{b,j}S_{b,j}$ , an urban-area based path loss expression  $PL_{b,j} = \beta_0 d_{b,j}^{-\gamma}$  is employed with  $\beta_0 \approx 1.35 \times 10^7$  and  $\gamma = 3$  [19], while shadow fading  $S_{b,j}$  is simulated with  $\sigma = 8dB$ .

Four schemes are simulated: 1. Conventional single user detector (5); 2. The optimal multiuser receiver in [8]; 3. JT-Decomp (25) with pre-compensation; 4. JT-Decomp without pre-compensation. Identical power constraint for each BS is assumed, with transmit SNR 25dB at each BS. Note that due to the path loss, the received SNR associated with the in-cell signal for MS at the cell borders will be weak and comparable with the interfering signals. For conventional single-cell signaling schemes (Schemes 1 and 2), a mobile user selects its associated BS with the largest path gain including the shadowing effect, and the power constraint at each BS is equally allocated to the in-cell users; while for the other two BS cooperation schemes, we use (20)~(21) to realize the power allocation. In Scheme 4, with synchronization concerns, if  $d_{b,j} - d_{b',j} < \Delta$ , which corresponds to the case when user  $j$  is located around point **A** or the cell borders (bold solid lines) in Figure 5, we can add BS  $b$  to the BS set of MS  $j$  denoted as  $\beta_j$ . We assume that signals transmitted from base stations in  $\beta_j$  can be synchronously received at MS  $j$ , so JT-

Decomp is applied only if more than one users have the same BS set. Otherwise single user eigen-beamforming at cooperative base stations within  $\beta_j$  is implemented. On the other hand, joint transmission can always be conducted regardless of MS locations for Scheme 3. Also for comparison, an interference-free scenario is drawn with the same per-user power as in Schemes 1 and 2, which unrealistically assumes that the signals for three users each with single-cell signaling are orthogonal, so that they do not interfere with each other and the per-user rate is similar to (6).

Figure 6 shows the cumulative distribution functions (CDF) of the throughput for these schemes. We can find that the advantage of BS cooperation (scheme 3) is still significant, although reduced a little from the strong CCI case in Figure 2. Scheme 3 performs worse than the interference-free case because of its transmit power inefficiency. Scheme 4 with  $\Delta = 300m$  performs almost the same as scheme 2. Note that based on our parameter setting, for most of the cases JT-Decomp cannot be implemented. However, in practical urban cellular systems, where  $N_t$  is much larger than  $N_r$  and more users can be processed simultaneously, the chance of BS cooperation will get larger, so it is expected that Scheme 4 will perform much better. Given the above analysis, together with the fact that Scheme 2 is not practical for MS, joint transmission without pre-compensation still assumes substantial advantages over single-cell signaling schemes.

For comparison, we assume another case, in which three users are uniformly distributed within 500m around point A in Figure 5. In this scenario, average CCI becomes much stronger and BS cooperation can be applied with a much higher chance for Scheme 4, resulting in the prominent performance gain of Scheme 4 over Scheme 2, as shown in Figure 7. Note that Scheme 3 now outperforms the interference-free case because of the increased power gain, as discussed in Section IV. A. From the above observations, as joint transmission is most beneficial for strong CCI scenario, in reality we can assign different sets of channels to near users (e.g., within 500m of a BS) and far users (beyond 500m), so they don't interfere with each other. We apply joint transmission only to the far co-channel users and go back to traditional transmission and detection for the near users. This scheme is especially applicable for indoor wireless access, which does not involve much mobility.

Therefore, we can conclude that BS cooperation schemes, either with or without pre-compensations, exhibit great advantage over single-cell schemes in realistic cellular applications, especially when CCI is strong.

## VIII. Conclusions

In this paper, cooperative processing at multicell base stations is introduced to address problems inherent on the downlink of cellular multiuser MIMO communications. In particular, the capability for co-channel interference cancellation, power gain, channel rank/conditioning advantage, and macro-diversity protection for BS cooperation are illustrated and verified. Although these advantages may not be

achieved simultaneously and may compete with each other, there is still an optimistic prediction on overall system performance improvement, which reveals the great potential of base station cooperative processing on meeting the ever-increasing capacity demands for wireless communications.

## APPENDIX

### A. Extension of LP-DP Approach in [21] to Multicell MIMO Vector BC Scenario:

If  $K = N_b$ , with the LQ decomposition of  $\mathbf{H}_T$ ,

$$\mathbf{H}_T = \begin{bmatrix} \mathbf{H}_{E1} \\ \mathbf{H}_{E2} \\ \vdots \\ \mathbf{H}_{EK} \end{bmatrix} = \mathbf{L}\mathbf{Q} = \begin{bmatrix} \mathbf{L}_{1,1} & & & \\ \mathbf{L}_{1,2} & \mathbf{L}_{2,2} & & \\ \dots & \dots & \dots & \dots \\ \mathbf{L}_{1,N_b} & \dots & \dots & \mathbf{L}_{N_b,N_b} \end{bmatrix} \mathbf{Q}, \quad (\text{A1})$$

where  $\mathbf{L}$  is lower triangular and  $\mathbf{Q}$  is unitary, and each block  $\mathbf{L}_{i,j}$  is a  $N_r \times N_t$  sub-matrix. We can get

$$\mathbf{H}_{Ej} = [\mathbf{L}_{1,j}, \mathbf{L}_{2,j}, \dots, \mathbf{L}_{j,j}, \mathbf{0}, \dots, \mathbf{0}] \mathbf{Q} \quad . \quad (\text{A2})$$

By defining  $\mathbf{v} = \mathbf{Q}\mathbf{T}\mathbf{s}_{[j]} = [\mathbf{v}_1^T, \mathbf{v}_2^T, \dots, \mathbf{v}_K^T]^T$ , (4) can be re-written as a virtual vector BC:

$$\mathbf{y}_j = [\mathbf{L}_{1,j}, \mathbf{L}_{2,j}, \dots, \mathbf{L}_{j,j}, \mathbf{0}, \dots, \mathbf{0}] \mathbf{v} + \mathbf{n}_j. \quad (\text{A3})$$

where sub-matrix  $\mathbf{L}_{j,j}$  represents the virtual channel matrix through which virtual signal  $\mathbf{v}_j$  is transmitted to MS  $j$ ; and  $\mathbf{L}_{i,j}$  represents the virtual interfering channel matrix from ‘previous’ users. With DPC, if the encoder of user  $j$  knows the non-causal virtual sequences of interference from user 1 to  $j-1$ , the mutual information for user  $k$  is the same as if the interference does not exist at all [7]. Then we can get  $K$  virtual parallel and non-interfering subchannels as

$$\mathbf{y}_j = \mathbf{L}_{j,j} \mathbf{v}_j + \mathbf{n}_j, \quad 1 \leq j \leq K. \quad (\text{A4})$$

Each such virtual channel can be further decomposed into parallel sub-streams by SVD:

$\mathbf{L}_{j,j} = \mathbf{U}_j \mathbf{\Sigma}_j \mathbf{V}_j^H$ . With a similar approach as (13), the joint transmission matrix can be expressed as:

$$\mathbf{T}\mathbf{s}_{[j]} = \mathbf{Q}^H \mathbf{v} = \mathbf{Q}^H \begin{bmatrix} \mathbf{V}_1 \mathbf{\Lambda}_1 \mathbf{s}'_{1-j} \\ \mathbf{V}_2 \mathbf{\Lambda}_2 \mathbf{s}'_{2-j} \\ \vdots \\ \mathbf{V}_j \mathbf{\Lambda}_j \mathbf{s}_j \\ \vdots \\ \mathbf{V}_{N_b} \mathbf{\Lambda}_{N_b} \mathbf{s}'_{K-j} \end{bmatrix} \Rightarrow \mathbf{T} = \mathbf{Q}^H \begin{bmatrix} \mathbf{V}_1 \mathbf{\Lambda}_1 & 0 \dots & 0 \\ 0 \dots & \vdots & \vdots \\ 0 \dots & \dots & \mathbf{V}_{N_b} \mathbf{\Lambda}_{N_b} \end{bmatrix}. \quad (\text{A5})$$

The sum rate achieved by LP-DP is then given as in equation (21):

$$SR_{LPDP} = \sum_{j=1}^K \sum_{l=1}^{L_j} \log \left| 1 + \frac{P_{j,l} \lambda_{j,l}^2}{N_0} \right|, \quad (\text{A6})$$

where  $\lambda_{j,l}$  represents the  $l$ th non-zero singular value of the virtual channel  $\mathbf{L}_{j,j}$ , and  $P_{j,l}$  can be the result of water-filling or equal power allocation.

### B. The approximate 2 bps/Hz power gain in Figure 2:

We can compare Sato's bound and single-cell upper bound at high SNR. Because  $\mathbf{H}_T$  has full rank (rank=6), for Sato's bound, the average per-user rate approximation at high SNR is:

$$\begin{aligned} \frac{1}{K} SR_{Sato} &= \frac{1}{K} \sum_{l=1}^{\text{rank}(\mathbf{H}_T)} \log \left( 1 + \frac{P_l}{N_0} \lambda_l^2 \right) \approx \frac{1}{K} \sum_{l=1}^{\text{rank}(\mathbf{H}_T)} \log \left( \frac{P_l}{N_0} \lambda_{T-l}^2 \right) \\ &= \frac{\text{rank}(\mathbf{H}_T)}{K} \log \left( \frac{P}{\text{rank}(\mathbf{H}_T) N_0} \right) + \frac{1}{K} \sum_{l=1}^{\text{rank}(\mathbf{H}_T)} \log(\lambda_{T-l}^2) \end{aligned} \quad (\text{B1})$$

Similarly, the per-user rate for single-cell upper bound is:

$$\begin{aligned} R_{1\_single\ cell} &= \sum_{l=1}^{\text{rank}(\mathbf{H}_{b_{1,1}})} \log \left( 1 + \frac{P_l}{N_0} \lambda_{1-l}^2 \right) \approx \sum_{l=1}^{\text{rank}(\mathbf{H}_{b_{1,1}})} \log \left( \frac{P_l}{N_0} \lambda_{1-l}^2 \right) \\ &= \text{rank}(\mathbf{H}_{b_{1,1}}) \log \left( \frac{P}{\text{rank}(\mathbf{H}_{b_{1,1}}) N_0} \right) + \sum_{l=1}^{\text{rank}(\mathbf{H}_{b_{1,1}})} \log(\lambda_{1-l}^2) \end{aligned} \quad (\text{B2})$$

We have  $\text{rank}(\mathbf{H}_{b_{1,1}}) = 2$ ,  $\text{rank}(\mathbf{H}_T) = 6$ ,  $K = 3$ , and  $P_l = 3P$  in our simulation, therefore the first summands in (B1) and (B2) are equal, and the gap between them is then:

$$\begin{aligned} \frac{1}{K} SR_{Sato} - R_{1\_single\ cell} &= \frac{1}{K} \sum_{l=1}^{\text{rank}(\mathbf{H}_T)} \log(\lambda_l^2) - \sum_{l=1}^{\text{rank}(\mathbf{H}_{b_{1,1}})} \log(\lambda_l^2) \\ &\sim \frac{1}{K} \text{rank}(\mathbf{H}_T) \log \left( \frac{1}{\text{rank}(\mathbf{H}_T)} \sum_{l=1}^{\text{rank}(\mathbf{H}_T)} \lambda_{T-l}^2 \right) - \text{rank}(\mathbf{H}_{b_{1,1}}) \log \left( \frac{1}{\text{rank}(\mathbf{H}_{b_{1,1}})} \sum_{l=1}^{\text{rank}(\mathbf{H}_{b_{1,1}})} \lambda_{1-l}^2 \right) \\ &= 2 \log \left( \frac{24}{6} \right) - 2 \log \left( \frac{4}{2} \right) = 2 \text{ bits / s / Hz} \end{aligned} \quad (\text{B3})$$

given  $E \left( \sum_{l=1}^{\text{rank}(\mathbf{H}_T)} \lambda_{T-l}^2 \right) = E(\|\mathbf{H}_T\|_F^2) = 24$  and  $E \left( \sum_{l=1}^{\text{rank}(\mathbf{H}_{b_{1,1}})} \lambda_{1-l}^2 \right) = E(\|\mathbf{H}_{b_{1,1}}\|_F^2) = 4$  based on our parameter setting.

## References

- [1] P. W. Baier, M. Meurer, T. Weber and H. Troeger, "Joint transmission (JT), an alternative rationale for the downlink of time division CDMA using multi-element transmit antennas," *Proc. 2000 IEEE 6th Int. Symp. Spread Spectrum Techniques*, vol. 1, pp. 1-5, Parsippany, NJ, Sept. 2000.
- [2] R. S. Blum, J. H. Winters, and N. Sollenberger, "On the capacity of cellular systems with MIMO," *Proc. 2001 Fall IEEE Vehicular Technology Conf.*, vol. 2, pp. 1220 -1224, Atlantic City, NJ, Oct. 2001.
- [3] G. Caire, S. Shamai, "On the achievable throughput of a multiantenna Gaussian broadcast channel," *IEEE Trans. Information Theory*, vol. 49, no. 7, pp. 1691-1706, July 2003.
- [4] S. Catreux, P. E. Driessen and L. J. Greenstein, "Simulation results for an interference-limited multiple-input multiple-output cellular system," *IEEE Commun. Lett.*, vol. 4, no.11, pp.334-336, Nov. 2000.
- [5] D. Chizhik, G. J. Foschini, M. J. Gans and R. A. Valenzuela, "Keyholes, correlations, and capacities of multielement transmit and receive antennas," *IEEE Trans. Wireless Communications*, vol. 1, no. 2, pp. 361 -368, April 2002.
- [6] R. Choi, and R. Murch, "MIMO transmit optimization for wireless communication systems," *Proc. 1st IEEE International Workshop on Electronic Design, Test and Applications*, pp. 33-37, Jan. 2002.
- [7] M. Costa, "Writing on dirty paper," *IEEE Transactions on Information Theory*, vol. 29 no. 3, pp. 439 - 441, May 1983.
- [8] H. Dai, and H. V. Poor, "Asymptotic spectral efficiency of multicell MIMO systems with frequency-flat fading," *IEEE Trans. Signal Processing*, vol. 51, no. 11, pp.2976-2989, Nov. 2003.
- [9] H. Dai, A. F. Molisch, and H. V. Poor, "Downlink capacity of interference-limited MIMO systems with joint detection," *IEEE Trans. Wireless Communications*, vol. 3, no.2, pp. 442-453, Mar. 2004.
- [10] R. F.H. Fischer, C. Windpassinger, A. Lampe, and J. B. Huber, "MIMO precoding for decentralized receivers," *Proc. 2002 IEEE International Symposium on Information Theory*, pp. 496, June 30~July 5, 2002.
- [11] G. J. Foschini and M. J. Gans, "On limits of wireless communications in a fading environment when using multiple antennas," *Wireless Personal Communications*, vol. 6, no. 3, pp. 311-335, Mar. 1998.
- [12] A. Goldsmith, S. A. Jafar, N. Jindal, and S. Vishwanath, "Capacity limits of MIMO channels," *IEEE J. Select. Areas Commun.*, vol. 21, no. 5, pp. 684-702, June 2003.
- [13] H. Huang, H. Viswanathan, and G.J. Foschini, "Multiple antennas in cellular CDMA systems: transmission, detection, and spectral efficiency," *IEEE Trans. on Communications*, vol. 1, no. 3, pp. 383-392, July 2002.
- [14] M. T. Ivrlac, W. Utschick , and J. A. Nossek, "Fading correlations in wireless MIMO communication systems," *IEEE J. Select. Areas Commun.*, vol. 21, no. 5, pp. 819-828, June 2003.
- [15] S. A. Jafar, G. J. Foschini , and A. Goldsmith, "PhantomNet: exploring optimal multicellular multiple antenna systems," *Proc. 2002 Fall IEEE Vehicular Technology Conf. (VTC)*, vol. 1, pp. 261-265, Vancouver, Canada, Sept. 2002.
- [16] S. A. Jafar, and A. Goldsmith, "Transmitter optimization for multiple antenna cellular systems," *Proc. 2002 IEEE International Symposium on Information Theory*, pp. 50, 30 June-5 July 2002.
- [17] N. Jindal, S. A. Jafar, S. Vishwanath, and A. Goldsmith, "Sum power iterative water-filling for multi-antenna gaussian broadcast channels," *Conference Record of the Thirty-Sixth Asilomar Conference on Signals, Systems and Computers, 2002*, vol. 2, pp. 1518 -1522, Nov. 3-6, 2002.
- [18] N. Jindal, S. Vishwanath, A. Goldsmith, "On the duality of Gaussian multiple-access and broadcast channels," *Proc. 2002 IEEE International Symposium on Information Theory*, pp. 500, 30 June-5 July 2002.

- [19] T. S. Rappaport, *Wireless Communications: Principles and Practice*, Prentice-Hall PTR, NJ, 1996
- [20] H. Sato, "An outer bound on the capacity region of broadcast channel," *IEEE Trans. on Info. Theory*, vol. 24, pp. 374-377, May 1978.
- [21] S. Shamai and B. M. Zaidel, "Enhancing the cellular downlink capacity via co-processing at the transmission end," *Proc. 2001 Spring IEEE Vehicular Technology Conf.*, pp. 1745-1749, Rhodes, Greece, May 2001.
- [22] D. Shiu, G. J. Foschini, M. J. Gans and J. M. Kahn, "Fading correlation and its effect on the capacity of multielement antenna systems," *IEEE Trans. on Communications*, vol. 48, no. 3, pp. 502-513, March 2000.
- [23] Q. H. Spencer, and M. Haardt, "Capacity and downlink transmission algorithms for a multi-user MIMO channel," *Conference Record of the Thirty-Sixth Asilomar Conference on Signals, Systems and Computers*, vol. 2, pp. 1384-1388, Nov. 2002.
- [24] S. Verdu, *Multiuser Detection*, Cambridge, U.K.; Cambridge Univ. Press, 1998
- [25] H. Viswanathan, S. Venkatesan, and H. Huang, "Downlink capacity evaluation of cellular networks with known-interference cancellation," *IEEE J. Select. Areas Commun.*, vol. 21, no. 5, pp. 802-811, June 2003
- [26] K.-K. Wong; R. D. Murch, R.S.-K. Cheng, and K. B. Letaief, "Optimizing the spectral efficiency of multiuser MIMO smart antenna systems," *Proc. IEEE Conference on Wireless Communications and Networking*, vol. 1, pp. 426-430, Chicago, IL Sept. 2000.
- [27] A. D. Wyner, "Shannon-theoretic approach to a Gaussian cellular multiple-access channel," *IEEE Trans. on Inform. Theory*, vol. 40, no. 6, pp. 1713-1727, Nov. 1994.
- [28] W. Yu, W. Rhee, S. Boyd, and J. M. Ciofli, "Iterative water-filling for Gaussian vector multiple access channels," *Proc. 2001 IEEE International Symposium on Information Theory*, pp. 322, Washington, DC, 24-29 June. 2001.
- [29] W. Yu, "A dual decomposition to the sum power Gaussian vector multiple access channel sum capacity problem," *Proc. 2003 IEEE Conference on Information Sciences and Systems*, the Johns Hopkins University, March, 2003.

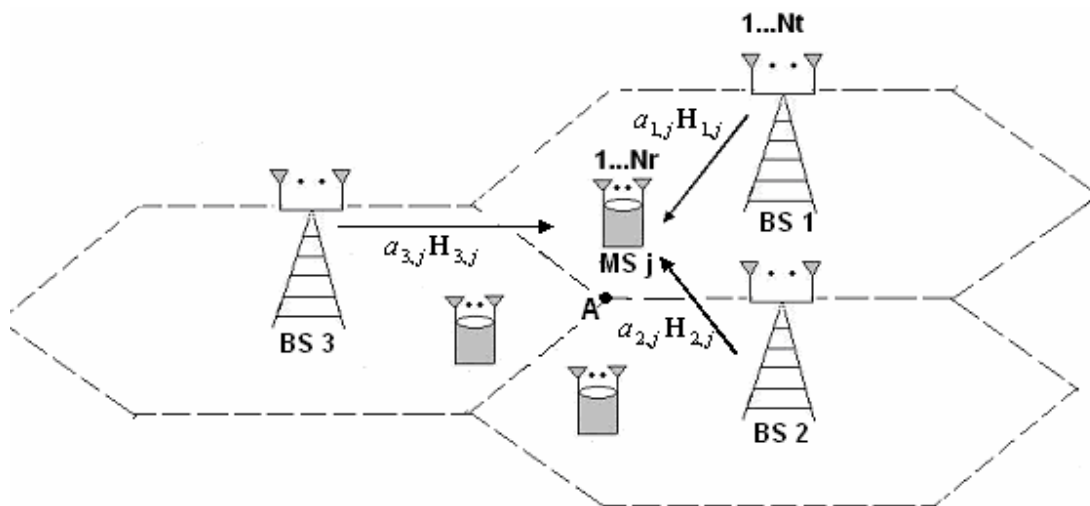
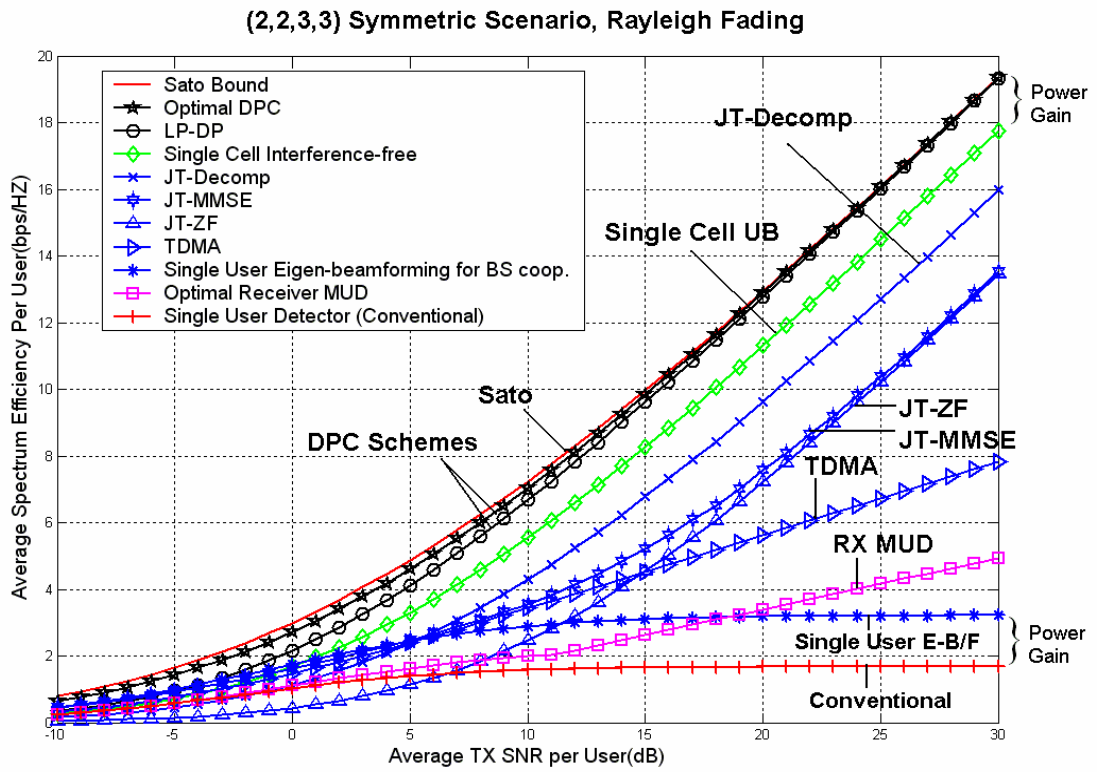
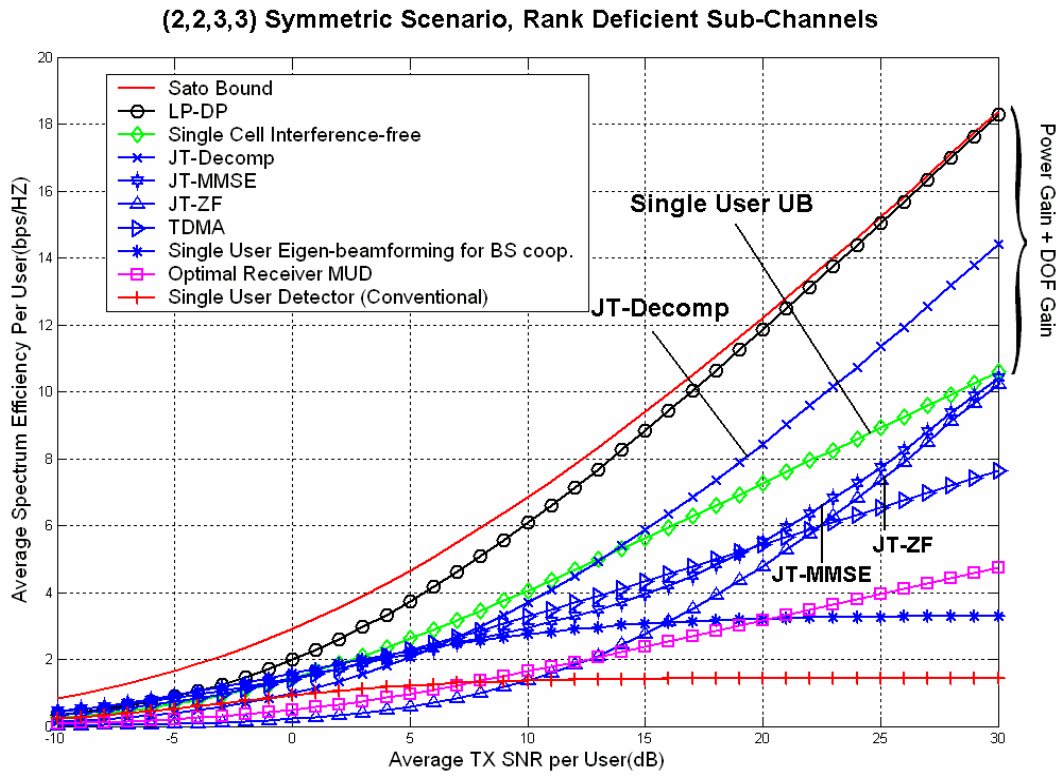


Figure 1. A multicell multiuser MIMO system with  $N_b = 3$ ,  $K = 3$



*Figure 2. Spectral efficiencies for Rayleigh fading*



*Figure 3. Spectral efficiencies for rank deficient channels*

(2,2,3,3) Symmetric Scenario, Rayleigh Fading with Shadowing

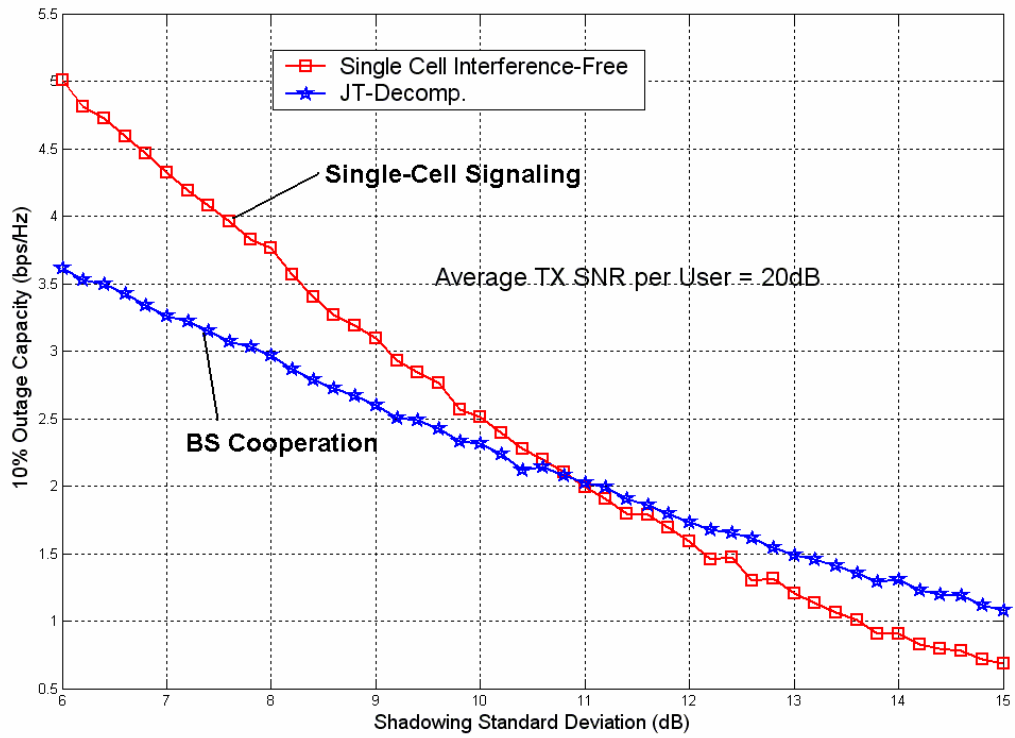


Figure 4. Spectral efficiencies for Rayleigh fading channels with shadowing

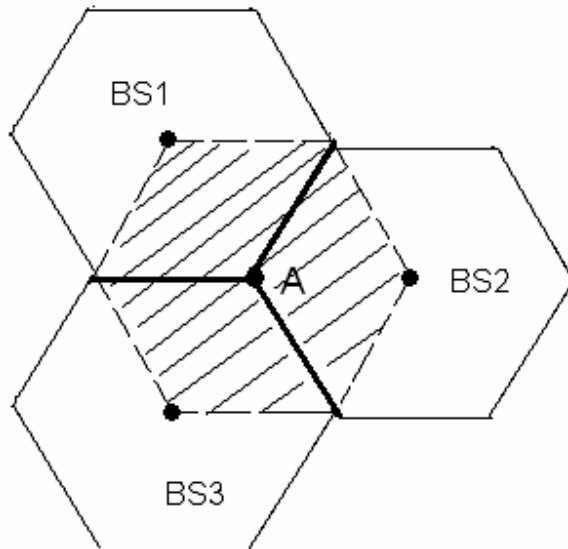


Figure 5. A realistic three-cell scenario

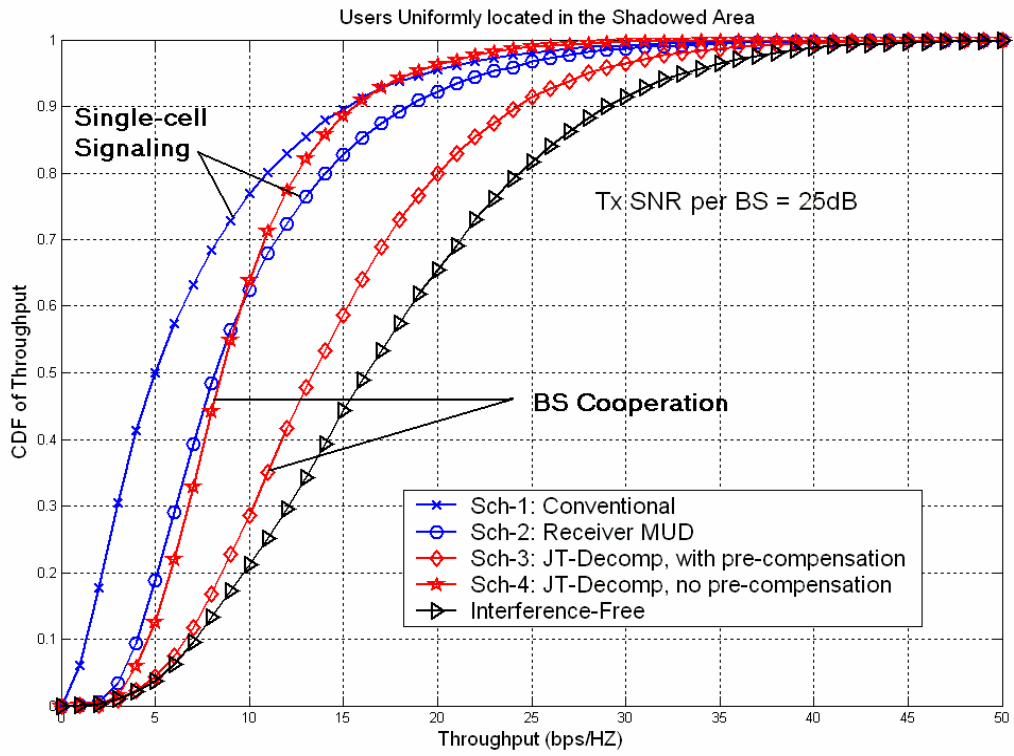


Figure 6. CDF's of scheme 1~4 for users uniformly located in the shadowed area of Figure 5

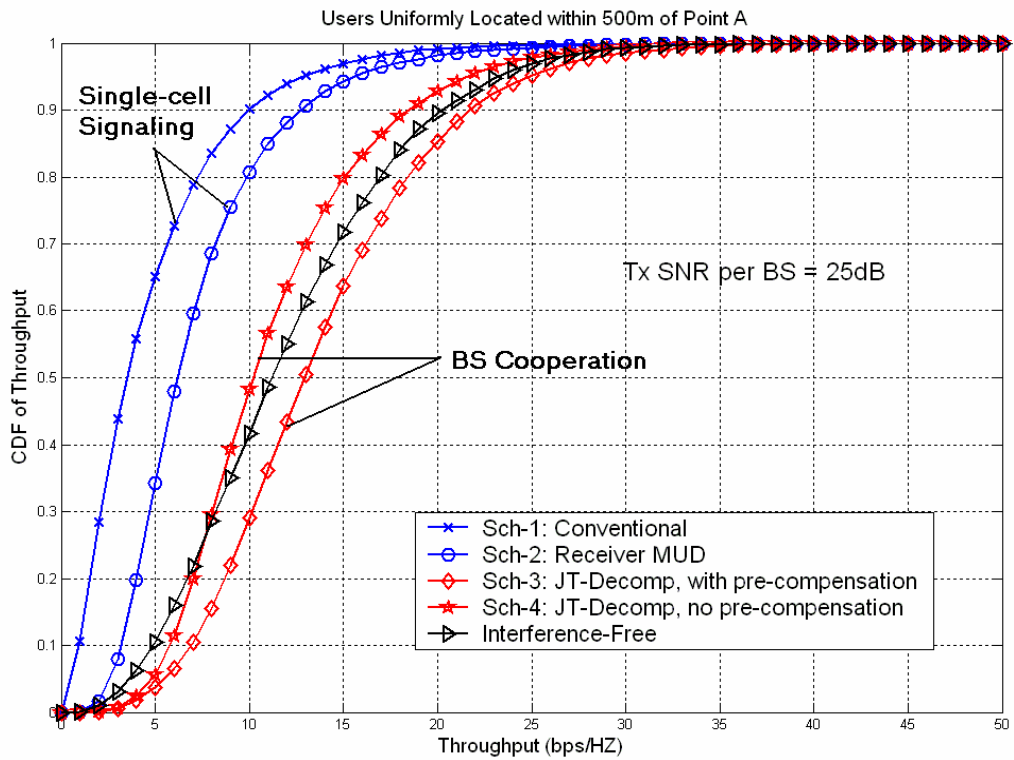


Figure 7. CDF's of scheme 1~4 for users uniformly located within 500m of point A in Figure 5